International Science and Technology Journal
المجلة الدولية للعلوم والتقنية
العدد 28
Volume 28
المجلة الدولية للعلوم والتقنية
ISTJ

The Effects of Sweep Angle and Sweep Location on the Performance of Helicopter Blades

[1]Hweda sharif, [2]Hamza Abobakar

[1]Technical College of Civil Aviation, Esbea, Libya

[2]College of Engineering Technology, Gharian

[1] hwedasharif@gmail.com, [2]almumonu2013@gmail.com

الملخص

الهدف من هذه الدراسة هو إجراء تحليل حدودي لمعرفة تأثير تكوينات ريش الطائرة المروحية المختلفة على أداء الدوار تحت ظروف التحويم. تتضمن التكوينات زوايا مسح مختلفة في مواقع امتداد مختلفة. تم تنفيذ الدراسة على حالة الاختبار وهي شفرة (Caradonna–Tung) الدوارة. البيانات أداء الدوار التي تم تحليلها هي قوة الدفع وعزم الدوران وشكل الجدارة. يتم إجراء جميع الحسابات عن طريق حل معادلات رينولدز متوسط نافير–ستوكس (RANS) مع نموذج اضطراب سبالارت ألماراس. أظهرت نتائج الدراسة أن زوايا المائلة الى الخلف و مواقعها المختلفة على شفرة (C–T) غير المدببة وغير الملتوية لها تاثير واضحا"على قوة الدفع وعزم الدوران، كما أن التأثير على عزم الدوران كان أكثر وضوحًا من التأثير على الدفع. ويلاحظ أن عزم الدوران قد ينخفض بحوالي 7٪ للشفرة (C–T) ويزيد FM في بعض الحالات.

الكلمات الدالة: شفرات دوار المروحية ، CFD ، حالة التحويم.

Abstract

The objective from this study is to carry out parametric analysis to know the effect of different helicopter blade configurations on the rotor performance under hover condition. The configurations include different sweep angles at different span locations. The study was implemented on test case which is, the Caradonna-Tung rotor blade. The analyzed rotor performance parameters are the

thrust, torque and figure of merit. All the computations are performed by solving the Reynolds Average Navier-Stokes (RANS) equations with the Spalart-Allmaras turbulence model. The results show that, the effect of different sweep angles and locations on the untapered and untwisted Caradonna-Tung (C-T) blade .Moreover, the effect on torque was much more pronounced than the effect on thrust. It is observed that the torque may decrease in around of 7 % for the C-T blade and increases FM in some cases.
Keywords: Helicopter rotor blade, CFD, hover condition.

1. Introduction.

The Computational Fluid Dynamics (CFD) has been extensively used in advanced aerodynamics that helps analyzing complex flow features. During the recent years, computational methods are increasingly becoming popular for determining the performances of various aeronautical designs. This technology has state-of-the-art capabilities, which minimize risk and assure low cost solutions to the existing challenges that aeronautical industry is confronting. Navier-Stokes solver helps finding a direct solution to the governing equations of the flow, and besides, it predicts the correct flow field even without requiring the airfoil load characteristics.

Still, it is difficult to analyze a rotor blade using CFD as compared to utilizing CFD for analyzing fixed wings [1, 6].

Egolf and Sparks [1] used finite difference solution method for the aerodynamic analysis of helicopter rotors .

Deesef and Agarwal [2] solved Euler's equations pertaining to the rotating coordinate system based on the blades' body-conforming curvilinear grids, and discussed them during the hovering condition. The adaptive CFD technique computes rotor-blade aerodynamics. Mustafa et al. have thrown light on it in their study [3].

Mark Potsdam et al. [4] experimented with fluid dynamic code and the rotorcraft computational structural dynamics (CSD) that calculates helicopter rotor air-loads under varying flight conditions.is useful for all the helicopter speeds and it accurately determines/predicts the 3-D flow characteristics .

Ilkko et al. [5] conducted simulations based on Reynolds-averaged Navier-Stokes equations, which they solved based on the available data of the UH-60A helicopter. The computations were conducted for validating FINFLO flow solver applying several turbulence models.

Chen et al. developed 3D Euler's solver following the finite volume upwind scheme for calculating the flow fields of the helicopter rotor blade during a forward flight [6].

Piotr D and Oskar S [7] have proven that a numerical method implemented in the SPARC code is capable of predicting flow field of a hovering Caradonna-Tung rotor during the transonic conditions.

Elfarra M.et al. [8] studied the effect of parabolic chord distribution and the taper stacking point location along the span of a helicopter rotor blade, which was analyzed in terms of the rotor thrust, torque and the figure of merit of the baseline Caradonna-Tung [12]

The rotor hover performance was predicted using CFD methods and simulations for the Helicopter Multi-block (HMB2), and it was validated for the Caradonna and Tung rotor during the hovering position. The overall results show excellent agreement with the experimental data, which means that the CFD is adequate for resolving the loads and handling the wake structure [9].

Patrick M. Shinoda [10] evaluated NASA Ames 80x120 feet wind tunnel for hover testing. He compared the rotor performance data with the predicted data, flight data of UH-60 aircraft and UH-60 model-scale data, and all the data showed good agreement when compared to the full-scale data.Choi et al. [11] used time-spectral and discrete adjoint-based methods for optimization of UH-60 rotor blade reducing torque without losing thrust.

In this study, the effects of different sweep angles, sweep angle location configurations on the performance of helicopter rotor blades are investigated. The baseline blades are the untwisted, untapered Caradonna &Tung (T.C). All the computations are performed by solving the Reynolds Average Navier Stokes (RANS) equations with implemeting the Spalart-Allmaras turbulence model.

2. Flow Solver and Validation Cases.

2.1 Flow solver.

This paper discusses the outcomes of the simulations of 3-D steady state Computational Fluid Dynamics (CFD) by presenting test case. The Caradonna-Tung, which was used in the testing facility of the Army Aero-mechanics Lab for conducting hovering tests. At the facility area, there was a large wind tunnel that was specifically designed with ducts to eliminate the re-circulation of air. The test case was considered for validating the commercial NUMECA CFD software.

The standard 3D RANS equations in a rotating frame of reference is as follows:

$$\frac{\partial}{\partial t}\int_V Q\,dV + \oint_S (F.\,n)dS - \oint_S (F_v.\,n)dS = \int_V S_T\,dV \qquad (1)$$

Where: **Q** is the vector of conservative variables, **F** is the invicid flux, $\mathbf{F_v}$ is the viscous flux and S_T is the source term. Those vectors are given by:

$$Q = \begin{Bmatrix} \bar{\rho} \\ \bar{\rho}\,\tilde{u}_1 \\ \bar{\rho}\,\tilde{u}_2 \\ \bar{\rho}\,\tilde{u}_3 \\ \bar{\rho}\,\tilde{e}_0 + k \end{Bmatrix} \qquad (2)$$

$$\boldsymbol{F} = \begin{Bmatrix} \bar{\rho}\,\widetilde{w}_j \\ \bar{\rho}\,\widetilde{w}_1\widetilde{w}_j + \bar{p}\delta_{1j} \\ \bar{\rho}\,\widetilde{w}_2\widetilde{w}_j + \bar{p}\delta_{2j} \\ \bar{\rho}\,\widetilde{w}_3\widetilde{w}_j + \bar{p}\delta_{3j} \\ \bar{\rho}\,\bar{h}_0\widetilde{w}_j + k\,\widetilde{w}_j \end{Bmatrix}, \quad \boldsymbol{F_v} = \begin{Bmatrix} 0 \\ \tilde{\tau}_{1j} - \tau_{1j}^T \\ \tilde{\tau}_{2j} - \tau_{2j}^T \\ \tilde{\tau}_{3j} - \tau_{3j}^T \\ \tilde{u}_i\,\tilde{\tau}_{ij} - \tilde{q}_j + \Theta_j^T \end{Bmatrix} \qquad (3)$$

$$\mathbf{s_T} = \begin{Bmatrix} 0 \\ -\bar{\rho}(\boldsymbol{\omega} \times \mathbf{u}) \\ 0 \end{Bmatrix} \quad (4)$$

Where w is the relative velocity, u is the absolute velocity, ρ is the density, e_o is total energy, p is the pressure, h_o is total enthalpy, k is the kinetic energy of turbulent fluctuations, τ_{ij}^T is the Reynolds stress tensor, θ_j^T consists of the turbulent heat flux tensor q_j^T and other turbulent terms evolving from density-velocity correlations and triple velocity correlations of the turbulent fluctuations, δ_{ij} is the Kronecker delta and ω is the angular velocity.

2.2. Caradonna-Tung Rotor Blade.

The test case is the Caradonna-Tung (1981) helicopter rotor [12]. This rotor has two untwisted and untapered blades.

Those blades had NACA 0012 profile. The aspect ratio is 6, the model rotor diameter is 2.286m, and the length of fixed chord along the span is 0.1905m. The real of the blade is shown in Figure.1.

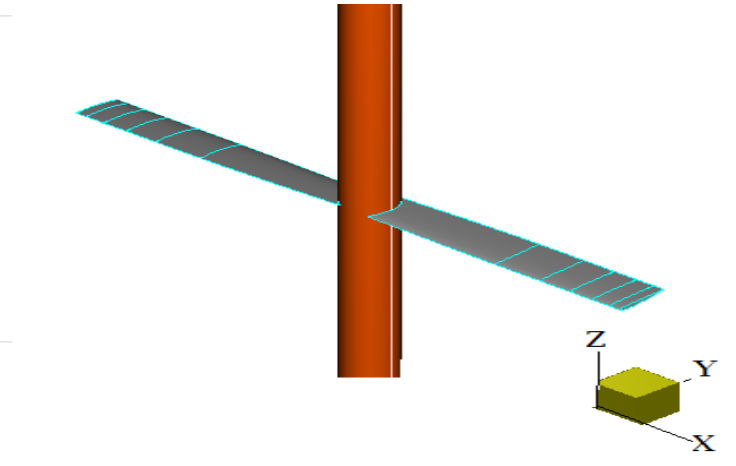

Figure 1. Caradonna-Tung blade geometry.

A mesh study for Caradonna-Tung rotor blade was performed. The Numeca AutoGrid structured mesh generator was used for

generating the mesh. The mesh was generated for a single blade under periodic conditions to account for the other blade. The mesh study was conducted at 2500 RPM rotational speed. Three mesh levels were investigated with resolutions of 131427, 965334 and 7391004 nodes. Table 1 summarizes the different grid levels used in the mesh study and the time taken for one convergent solution.

Table1. Mesh study for Caradonna-Tung rotor.

Mesh name at hover	Number of nodes	Run Time
Coarse	**131427**	**1 hr**
Fine	**965334**	**3 hr**
Finer	**7391004**	**12 hr**

The pressure coefficient distributions at r/R = 0.96 spanwise locations along the blade is validated against the experimental data for the three grid levels as shown in Figure 2.

By looking at the results in Table 1 and Figure 2, it was found that the fine mesh passes through the experimental solution points more conveniently as compared to the other forms. From this observation, it was concluded that the fine mesh will be used for all the computations.

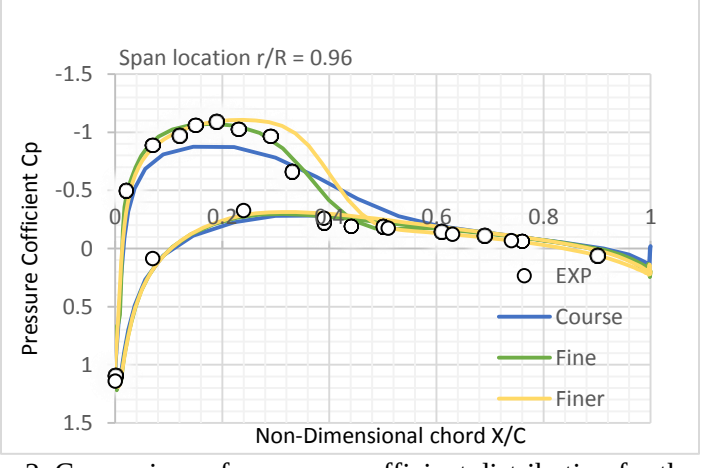

Figure 2. Comparison of pressure coefficient distribution for the three grid levels.

3. Parametric Study

As mentioned before, the Caradonna-Tung blade was chosen for the parametric study. The shape of blade and its tip are significant for the helicopter's aerodynamic performance. The blade tips encounter the peak pressure and high Mach number while strong trailing tip vortices are produced.

A poor tip design causes serious implications for the performance of a rotor. In this section, the changes in the shape of the blades will be discussed in this part will analyze the effect of the blades' sweepback angle on the rotor performance under the hovering condition.

3.1. Sweep angle and sweep location for Caradonna Tung.

Various blade configurations based on different sweep angle values and different spanwise sweep locations have been produced. The considered sweep locations are: 80%, 90%, 92%, 94%, 95% and 96% in the spanwise direction. And the studied sweep angles are 30, 40, 50, 60 and 80 degrees. Two cases are shown in Figure 3.

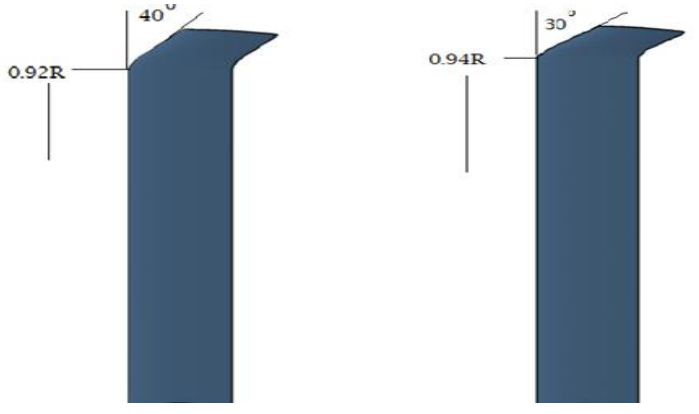

Figure 3. Sweep angle and sweep locations.

The analysis was carried out under a rotational speed of 2500 RPM and a collective pitch angle of 8 degrees during the hovering condition.

Calculating the percentage of increase in thrust and the percentage of decrease in torque and also the figure of merit (FM)

for sweepback angle configurations is significant in determining the rotor performance. The figure of merit is defined in Equation 5.

$$1.\ FM = \frac{C_T^{3/2}}{\sqrt{2}C_Q} \qquad (5)$$

where C_T and C_Q are the thrust and torque coefficients respectively.

Higher thrust generation is better for the hovering condition. However, more torque generation means that more power is needed to attain that thrust, which makes the helicopter less efficient.

The results in terms of percentage of increase in thrust, percentage of decrease in torque and percentage of increase in figure of merit with respect to the baseline blade are listed in Table 2.

Table 2. Results for different Caradonna Tung configurations.

Sweep Angle (deg.)	Sweep Location r/R (%)	FM (%)	Thrust (%)	Torque (%)
30	94	8.967	0.760	6.985
	96	7.065	0.253	6.123
40	92	9.239	1.171	6.551
	94	8.152	0.984	6.049
	96	5.978	0.228	5.169
50	92	7.337	1.034	5.268
	94	6.522	0.673	4.880
60	80	0.272	-0.929	1.354
	90	1.359	-3.091	5.572
	92	5.435	0.587	4.083
	94	4.620	0.231	3.914
	95	3.533	-0.281	3.615
	96	3.533	-0.284	3.615
80	90	1.902	-0.482	2.492
	94	1.902	-0.649	2.591

The results show that the effect of the sweep angle and location is more pronounced on the torque reduction than on thrust

increase. An increase in FM of more than 9% is possible when the sweep angle is 40 degrees and the sweep location is at 92% along the blade span.

The pressure coefficient at different spanwise locations are plotted for the sweptback angles of 30° and 40° located at 94% and 92% span respectively and compared with the baseline blade at 2500 RPM as shown in Figure 6. The pressure coefficient was found to be different as compared to the baseline blade. This difference becomes clearer towards the blade tip section where the sweep occurs. The difference in pressure coefficient explains the changes in the thrust and torque values.

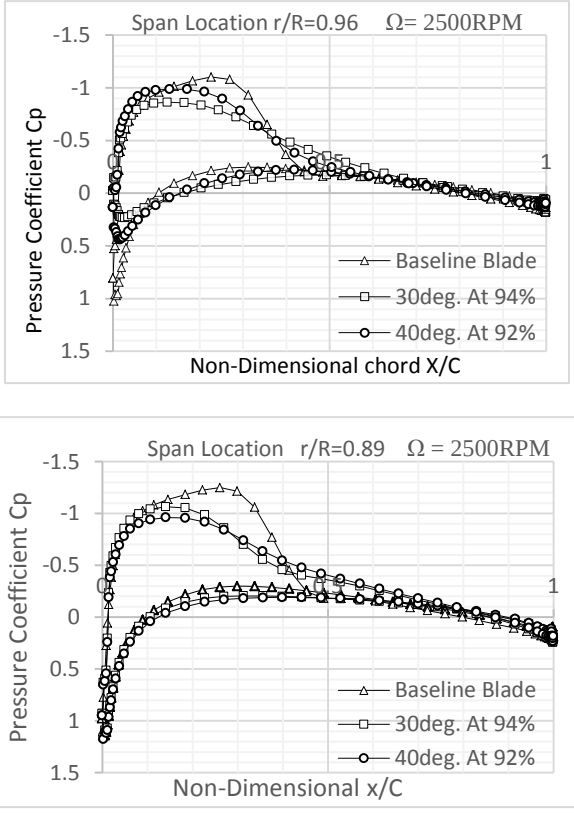

Figure 4. Comparison of pressure coefficient distribution for different cases of Caradonna Tung.

4. Conclusion.

In this study, the parametric analysis of the untwisted and untapered Cardonna-Tung, rotor blade was conducted using CFD .

Different blade configurations were generated based on changing the sweep angle and the spanwise location.

The effect of the produced geometries on the blade performance in terms of thrust force, torque and figure of merit was studied.

The results have shown that the effect of sweep angle and spanwise location is much more pronounced in the case of the untwisted C-T blade. Around 7% decrease in torque and 9% increase in FM was possible for some cases of C-T blade.

5. References.

[1]. Egolf T. A. and Sparks S. P., "A Full Potential Flow Analysis with RealisticWake In uence for Helicopter Rotor Airload Prediction," NASA CR-4007, 1987.

[2]. Agarwal R. K. and Decse J. E., "Euler Calculations for a Flow eld of a Helicopter Rotor in Hover," *Journal of Aircraft*, Vol. 24, No. 4, pp. 231-238, 1987.

[3]. Mustafa D., Mark S. S., Joseph E. F., Kenneth J., "Adaptive CFD analysis for rotorcraft aerodynamics", Scientific Computation Research Center, Rensselaer Polytechnic Institute, Troy, NY 12180, USA,1999.

[4]. Potsdam M., Yeo W., Johnson W. ,"Rotor airloads prediction using loose aerodynamic structural coupling," *American Helicopter Society*, 60th Annual Forum, Baltimore, MD, 7–10 June 2004.

[5]. Juho Ilkko, Jaakko Hoffren and Timo Siikonen," Simulation of a helicopter rotor flow," *Journal of Structural Mechanics*, Vol. 44, No 3, pp. 186 – 205, 2011.

[6]. Chen C.L., McCroskey W.J. and Obayashi S." Numerical solutions of forward-flight rotor flow using an upwind

method," *Journal of Aircraft*, Vol. 28, No. 6, pp. 374-380, 1991

[7]. Piotr Doerffer and Oskar Szulc," Numerical Simulation Of Model Helicopter Rotor In Hover," Institute of Fluid-Flow Machinery PAS, Fiszera 14, 80-952 Gdansk, Received 28 May 2008.

[8]. Elfarra M. and Kaya M., "CFD Analysis of the Effect of Parabolic Taper Distribution of an Untwisted Helicopter Rotor Blade", *Journal of Aeronautics and Space Technology*, Vol. 11, No. 2, pp. 59-70, 2018.

[9]. Nik Ahmad Ridhwan Nik Mohd and George N. Barakos, "Computational Aerodynamics of Hovering Helicopter Rotors," *Jurnal Mekanikal*, Vol. 34, pp. 16-46, 2012.

[10]. Shinoda P. M., Yeo H. and Norman, T. R., "Rotor Performance of a UH-60 Rotor System in the NASA Ames 80-by 120-Foot Wind Tunnel," Proceedings of the 58th Annual American Helicopter Society Forum, Montreal, Canada, June 11-13, 2002.

[11]. Seongim Choi, Kihwan Lee, Mark M. Potsdam and Juan J. Alonso, "Helicopter Rotor Design Using a Time-Spectral and Adjoint-Based Method," *Journal Of Aircraft*, Vol. 51, No. 2, pp. 412-423, 2014.

[12]. F.X. Caradonna and C. Tung, "Experimental and analytical studies of a model helicopter rotor in hover," NASA TM 81232, 1980.